Published in final edited form as:
Invest Radiol. 2010 October ; 45(10): 600–612. doi:10.1097/RLI.0b013e3181ee5a9e.

High relaxivity MRI contrast agents part 1: Impact of single donor atom substitution on relaxivity of serum albumin-bound gadolinium complexes

Stephane Dumas[a], **Vincent Jacques**[a], **Wei-Chuan Sun**[a], **Jeffrey S. Troughton**[a], **Joel T. Welch**[a], **Jaclyn M. Chasse**[a], **Heribert Schmitt-Willich**[b], and **Peter Caravan**[a,c,*]

[a]formerly with Epix Pharmaceuticals, Cambridge, MA, USA

[b]Bayer Schering Pharma AG, Berlin, Germany

[c]Athinoula A. Martinos Center for Biomedical Imaging, Massachusetts General Hospital and Harvard Medical School, 149 Thirteenth St, Suite 2301, Charlestown MA 02129

Abstract

Rationale and objectives—The donor atoms that bind to gadolinium in contrast agents influence inner-sphere water exchange and electronic relaxation, both of which determine observed relaxivity. These molecular parameters impact relaxivity greatest when the contrast agent is protein bound. We sought to determine an optimal donor atom set to yield high relaxivity compounds.

Methods—Thirty-eight Gd-DOTA derivatives were prepared and relaxivity determined in presence and absence of human serum albumin as a function of temperature and magnetic field. Each compound had a common albumin-binding group and differed only by substitution of different donor groups at one of the macrocycle nitrogens. O-17 relaxometry at 7.05T was performed to estimate water exchange rates.

Results—Changing a single donor atom resulted in changes in water exchange rates ranging across 3 orders of magnitude. Donor groups increased water exchange rate in the order: phosphonate ~ phenolate > α-substituted acetate > acetate > hydroxamate ~ sulfonamide > amide ~ pyridyl ~ imidazole. Relaxivites at 0.47T and 1.4T, 37 °C, ranged from 12.3 to 55.6 $mM^{-1}s^{-1}$ and from 8.3 to 32.6 $mM^{-1}s^{-1}$ respectively. Optimal relaxivities were observed when the donor group was an α-substituted acetate. Electronic relaxation was slowest for the acetate derivatives as well.

Conclusions—Water exchange dynamics and relaxivity can be predictably tuned by choice of donor atoms

Keywords

Relaxivity; gadolinium; protein binding; water exchange; NMRD

INTRODUCTION

Magnetic resonance (MR) imaging contrast agents are unique among diagnostic imaging probes in that the imaging agent is detected indirectly. The contrast agent catalytically relaxes solvent water hydrogen atoms that it encounters, and this relaxation enhancement

*to whom correspondence should be addressed: caravan@nmr.mgh.harvard.edu.

generates image contrast on T_1- or T_2-weighted images. The extent to which a contrast agent can affect the relaxation rate of tissue water ($1/T_1$ or $1/T_2$) is termed relaxivity (r_1 or r_2) and is given by equation 1, where [CA] is the concentration of the contrast agent.

$$\frac{1}{T_i}=\frac{1}{T_i^0}+r_i\,[CA]\;;i=1,2 \tag{1}$$

Tissue has an inherent relaxation rate ($1/T_1^0$), so in order to generate readily observable contrast the r_1[CA] product should be at least 10% of the inherent rate. For commercial extracellular fluid agents like Gd-DTPA, r_1 is on the order of 4 $mM^{-1}s^{-1}$ and as a result very large doses of contrast agent are required to affect T_1. Increasing relaxivity would enable contrast-enhanced MRI to be performed at lower doses and may lower the risk of gadolinium (Gd)-induced toxicity. The importance of gadolinium-associated toxicity has been recently emphasized by recognition of an association of Gd-based contrast agents with nephrogenic systemic fibrosis.[1-3] In addition to safety, molecular imaging is driving improvements in relaxivity.[4-7] For a targeted imaging agent, higher relaxivity would allow lower concentration targets to be detected by MRI. Unlike nuclear medicine where the number of photons emitted at a fixed radiochemical concentration is known and constant, relaxivity is not a static effect but depends on the molecular properties of the contrast agent.[8,9]

For gadolinium (Gd)-based contrast agents, relaxivity depends on extrinsic factors like applied field and temperature. It also depends on intrinsic factors such as the number of water molecules in the inner-coordination sphere (i.e. directly bonded to the Gd and denoted *q*), the mean residency time of such water molecules (τ_m whose inverse is the water exchange rate, $k_{ex} = 1/\tau_m$), the number of water molecules or exchangeable hydrogen atoms in the second and subsequent coordination spheres and their residency times, see Figure 1A. Gd-induced longitudinal relaxation is a dipolar process that depends on the gadolinium to hydrogen distance as the inverse 6th power (r_{GdH}^{-6}). In order to induce nuclear relaxation, the contrast agent creates a fluctuating magnetic field. This fluctuation can arise from the tumbling of the molecule in solution and for compounds tumbling isotropically this is described by a characteristic rotational correlation time, τ_R. The fluctuating field can also be a result of the electrons in the Gd^{3+} ion undergoing excitation and relaxation. At fields of 0.1T and higher, nuclear (hydrogen) relaxation is modulated by the longitudinal electronic relaxation time T1e. Electronic relaxation is also field dependent and $1/T_{1e}$ decreases with the square of increasing field. The mechanism for electronic relaxation is transient zero-field splitting (ZFS) modulation where ligand field about the Gd^{3+} ion is transiently distorted due to vibrations and solvent collisions resulting in electronic relaxation. The magnitude of this distortion is given by a term denoted Δ_t^2 (square of trace of ZFS tensor) and is modulated by a correlation time termed τ_v. The fluctuating field can also be a result of the water molecule coming into contact with the metal complex.

Relaxivity is obviously a complex phenomenon involving inner-sphere (r_1^{IS}) and outer-sphere (r_1^{OS}) mechanisms as explained above. Often the effect due to the inner-sphere water molecule(s) is factored out.[8,9] Inner-sphere relaxivity can be described by a two-site exchange model as shown in equation 2, where T_{1m} is the T_1 of the bound water molecule. At imaging fields of 0.1T and higher, the relaxation rate of the bound water is given by equation 3 where $1/T_{1m}$ depends on several physical constants (*C*), the Gd-water hydrogen distance (r_{GdH}), a correlation time for the magnetic fluctuation (τ_c), and the Larmor frequency (ω_H).[8] The correlation time for the magnetic fluctuation (τ_c) is a function of rotational, electronic and exchange correlation times. The shortest correlation time will dominate τ_c as shown by equation 4.

$$r_1 = r_1^{IS} + r_1^{OS} = \frac{q/[H_2O]}{T_{1m} + \tau_m} + r_1^{OS} \quad (2)$$

$$\frac{1}{T_{1m}} = \frac{C}{r_{GdH}^6}\left[\frac{3\tau_c}{1+\omega_H^2\tau_c^2}\right] \quad (3)$$

$$\frac{1}{\tau_c} = \frac{1}{\tau_R} + \frac{1}{T_{1e}} + \frac{1}{\tau_m} \quad (4)$$

For small molecules like Gd-DTPA at clinical field strengths, the relevant correlation time is always the rotational correlation time τ_R which is on the order of 50 – 200 ps at 37 °C.[10,11] When one computes T_{1m} for such small molecules it is always large (several microseconds) compared to the mean residency time of the water bound to Gd (typically sub-microsecond at 37 °C, so $T_{1m} >> \tau_m$). The GdH distance has been investigated by electron nuclear double resonance techniques and does not vary significantly amongst all the compounds studied.[12–14] As a result, for small molecules inner-sphere relaxivity is well approximated by equation 5 and depends only on the number of inner-sphere water (q) molecules and the rotational correlation time (τ_R), where C' is a constant, Figure 1B.

$$r_1^{IS} = C' \times q \times \tau_R \quad (5)$$

It is well known that increasing the rotational correlation time, e.g. by protein binding, will increase relaxivity.[9,15] As rotational motion is slowed, relaxivity will begin to be limited by other parameters (Figure 1C). For example τ_m becomes greater than T_{1m} in eqn 2 or T_{1e} or τ_m becomes the dominant correlation time in eqn 4. This represents a challenge in identifying new high relaxivity Gd complexes. Simply screening the complexes as small molecules will give results largely dependent on hydration number and molecular weight (proportional to rotational correlation time). While it is possible to measure τ_m and T_{1e} using other physical methods,[11,13,16–18] it is not obvious whether these parameters will be unchanged when the complex is targeted to a protein. For instance, it has been shown that water exchange can be slowed upon protein binding[19,20] and electronic relaxation may be overestimated in small molecules.[21,22]

In this report we describe an approach to identifying high-relaxivity Gd chelates by using a common framework based on the thermodynamically stable GdDOTA complex. Each of the complexes has a common, high affinity serum albumin binder attached via a substituted acetate. One donor group at N7 in the cyclen ring (Figure 2) is varied to explore the effect of donor group on water exchange kinetics, second-sphere hydration, and electronic relaxation and its cumulative effect on relaxivity. The compounds are screened by measuring relaxivity at 0.47 and 1.4T in the presence (immobilized) and absence of human serum albumin. A subset of the complexes are further studied by variable temperature proton nuclear magnetic relaxation dispersion (NMRD) and variable temperature O-17 relaxometry, and the data analyzed to extract the molecular determinants of relaxivity.

MATERIALS AND METHODS

Compound synthesis

Compounds **Gd2a**, **Gd3b** and **Gd6c** were described previously, [23,24] and the other compounds used in this report have been described in a patent application.[25] Here, the synthesis of the advanced intermediate used to prepare all the compounds is described in detail (see Figure 2 for scheme and numbering).

Synthesis of diisopropyl-phosphoramidous acid tert-butyl ester 2,5,2′,4′,6′-pentamethyl-biphenyl-4-yl ester, 13—was achieved using phosphorylation conditions described by Bannwarth.[26,27] Pentamethyl hydroxybiphenyl **12** was synthesized as described previously.[28] Biphenyl **12** (3.55 g, 14.8 mmol) was dissolved in anhydrous acetonitrile (40 ml) and tert-butyl tetraisopropylphosphorodiamidite (5.94 g, 19.5 mmol, 1.3 eq.) was added at once. Diisopropylammonium tetrazolide[29] (3.80 g, 22.2 mmol, 1.5 eq.) was added at once under argon at room temperature (RT). The reaction was monitored by ^{31}P NMR (136.1 ppm: starting material and 131.9 ppm: product) and by thin layer chromatography (TLC). After 5h the solvent was evaporated and the residue was triturated with ether (100 mL). The white precipitate was filtered off and was rinsed with ether (2 × 25 mL). Evaporation of ether gave 8.77 g of crude phosphoramidite, which was purified by short flash chromatography on silica gel (ethyl acetate(EtOAc)/hexane(Hex) 9:1 to 8.5:1.5 to 4:1) to give 6.00 g (92%) of desired phosphoramidite as a white solid.

Synthesis of (S)-5-[tert-Butoxy-(2,5,2′,4′,6′-pentamethyl-biphenyl-4-yloxy)-phosphoryloxy]-2-hydroxypentanoic acid tert-butyl ester, 14—(S)-2,5-dihydroxypentanoic acid tert-butyl ester[30,31] (0.79 g, 4.2 mmol, 1 eq.) and phosphoramidite **13** (1.66 g, 3.7 mmol, 0.9 eq.) were dissolved in 1:2 mixture of acetonitrile/methylene chloride (12 mL) and 4Å molecular sieves (3.5 g) were added under argon. 3% 1*H*-Tetrazole in acetonitrile (0.32 g, 4.6 mmol, 1.1 eq.) was added at once at –40°C and the reaction mixture was stirred for 4h between –40°C and 15°C. The reaction was monitored by ^{31}P NMR (136.5 ppm, s: starting material and 131.0 ppm, d: product). *tert*-Butylhydroperoxide (1.15 mL, 8.3 mmol, 2eq.) was added and the oxidation was complete (^{31}P NMR: -12.8 ppm) in 40 minutes. The molecular sieves and the white solid formed were filtered off and the filtrate was diluted with EtOAc (100 mL) then washed successively with 10% sodium bisulfite ($Na_2S_2O_3$) twice, with saturated sodium hydrogenocarbonate ($NaHCO_3$) and with brine. The organic layer was dried over sodium sulfate (Na_2SO_4). Evaporation of solvents gave 3.06 g of crude phosphotriester as an orange-yellow oil that was purified by flash chromatography on silica gel (1% triethylamine in Hexanes/EtOAc 3:1 to 1:1) to give 1.75 g (85%) of desired phosphotriester **14** as a racemic mixture at the phosphorus center.

Synthesis of (S)-5-[tert-Butoxy-(2,5,2′,4′,6′-pentamethyl-biphenyl-4-yloxy)-phosphoryloxy]-2-(4-nitrobenzenesulfonyloxy)-pentanoic acid tert-butyl ester, 15—Compound **14** (2.16g, 3.9 mmol) was dissolved in methylene chloride (50 mL) and triethylamine (1.0 mL, 7.2 mmol, 1.8 eq.) was added at once. 4-Nosyl chloride (2.50 g, 11.3 mmol, 2.9 eq.) was added at once at 0°C and the solution was stirred for 1h at 0°C and was warmed to RT in 2 h. The reaction mixture was washed with saturated $NaHCO_3$ and the organic layer was dried over Na_2SO_4. Evaporation of solvent gave the crude nosylate as an orange oil, which was purified by flash chromatography on silica gel (0.1% Et_3N in Hexanes / EtOAc 9:1 to 3:1) to give 2.26 g (78%) of desired nosylate **15** as a foaming white solid.

Synthesis of 2-(4,10-Bis-tert-butoxycarbonylmethyl-1,4,7,10-tetraaza-cyclododec-1-yl)-5-(R)-[tertbutoxy-(2,5,2′,4′,6′-pentamethyl-biphenyl-4-yloxy)-

phosphoryloxy]-pentanoic acid tert-butyl ester, 16—1,7-DO2A bis-(tert-butyl ester) (2.29 g, 5.7 mmol, 2 eq.) was obtained from Macrocyclics (Dallas, TX) and dissolved in anhydrous acetonitrile (10 mL) and potassium carbonate (K_2CO_3) (0.79 g, 5.72 mmol, 2 eq.) was added under argon. Nosylate **15** (2.10 g, 2.9 mmol, 1 eq.) dissolved in acetonitrile (6 mL) was added dropwise over 50 minutes at room temperature. The mixture was stirred for 25 h and the acetonitrile was evaporated. The residue was triturated in ether (50 mL) and the solid was filtered off. The ether layer was washed successively with 0.5% citric acid (2 × 50 mL), saturated $NaHCO_3$ (50 mL) and with brine (50 mL). The organic layer was dried over Na_2SO_4. Evaporation of solvent gave 2.37 g of a 8:1 mixture of desired mono phosphate and bis phosphate that was used directly in the next step without any further purification. The pH of the citric acid extracts was adjusted to 9 with saturated $NaHCO_3$ and then the aqueous layer was extracted with EtOAc (4 × 30 mL). The combined organic fractions were washed with brine (30 mL) and dried over Na_2SO_4. Evaporation of solvent gave 0.86 g of recovered 1,7-DO_2A bis-(tert-butyl ester). MS monophosphate: [M+1]= 931.5; bisphosphate: [M+1]= 1461.7

Synthesis of Gd1g—Alkylation conditions varied depending on the donor group being introduced. However all deprotection and chelation reactions followed a common procedure. Here the synthesis of **Gd1g** is given as an example. Advanced intermediate **16** (100 mg, 0.11 mmol, 1 eq) and dimethyl bromomalonate (36 mg, 0.17, 1.5 eq.) were dissolved in acetonitrile (0.5 mL). Diisopropylethylamine (40 mL, 0.22 mmol, 2 eq.) was added and the solution was stirred at RT for 24h. The solvent was evaporated under reduced pressure. The residue was re-dissolved in EtOAc. The organic layer was washed successively with water and brine and was dried over Na_2SO_4. The solvent was removed under reduced pressure to give the desired crude protected ligand **1g**. MS: [M+1] = 1061.7 The protected ligand (**1g**) was dissolved in trifluoroacetic acid (TFA)/methanesulfonic acid/phenol (95:2.5:2.5, 2 mL) and the reaction stirred at RT for 2 hr to remove the t-butyl groups. TFA was evaporated and the residue was suspended in water. The pH was adjusted to 12 with 1N NaOH to saponify the ethyl esters. The reaction was monitored by LC-MS. After 4h the reaction mixture was lyophilized to give the crude ligand (**1g**) as a brown solid. MS: [M+1] = 787.4.

The ligand (**1g**) was dissolved in H_2O and the pH adjusted to 6 with a 1N NaOH solution. A 245 mM solution of $GdCl_3$ was added (1 eq based on ligand weight) and the pH adjusted to 6. The reaction mixture was stirred at 45°C for 5 hours and the chelation monitored by LC-MS. EDTA solution was added to chelate the excess Gd^{3+} and the product was purified by preparative-HPLC on a C-18 column using a gradient of 50 mM aqueous ammonium formate and acetonitrile. After lyophilization of the pure fractions, **Gd1g** (16 mg) was obtained. MS: [M+1] = 961.2 with expected isotopic mass distribution.

Sample preparation and concentration determination

Human serum albumin (Fraction V, Sigma) was dissolved in 50 mM HEPES buffered saline (HBS) of 150 mM sodium chloride content (pH 7.4) to reach a final protein solution of ~6% (w/v). Protein concentration was estimated from absorbance at 280 nm compared to a series of albumin standards (Sigma). This stock solution was used to prepare 4.5% (w/v) HSA solutions (0.67 mM) by appropriate dilution with a gadolinium chelate stock solution (5 – 10 mM) and HBS. For relaxivity determinations, the Gd concentration ranged from 0 – 0.1 mM and for nuclear magnetic relaxation dispersion (NMRD) and protein binding studies the Gd concentration was 0.1 mM. All gadolinium concentrations were determined by inductively coupled plasma mass spectroscopy (ICP-MS) on an Agilent 7500a system.

Ultrafiltration Measurements of Protein Binding—Solutions of 0.1 mM Gd compound and 4.5% HSA (400 μL total) were added to a 5000 MW ultra-filtration unit

(regenerated cellulose membrane, Millipore, Bedford, MA). The samples were incubated at 37°C for thirty minutes, placed in pre-warmed centrifuge buckets and centrifuged for seven minutes at 3500G and 37°C using a Jouan GT 4 22 centrifuge. The filtrates were analyzed for gadolinium concentration by ICP-MS. The concentration of bound complex in the protein samples was determined by subtracting the gadolinium concentration (unbound complex) found in the filtrate from the gadolinium concentration of the initial solution. Experiments were performed in duplicate.

Relaxivity—Water proton relaxation rates ($1/T_1$ and $1/T_2$) were determined at 20 MHz (0.47 T) and 60 MHz (1.41 T) using a Bruker NMS 120 Minispec and a Bruker mq60 Minispec, respectively. Samples, 200 μL, were pipetted into glass vials and were equilibrated for at least 20 minutes at 37°C before being measured at 37°C. T_1 was measured with an inversion recovery pulse sequence using 10 different TI times; the pre-acquisition delay was always set to at least $5T_1$. T_2 was measured using a Carr Purcell Meiboom Gill (CPMG) sequence with 300 to 500 echoes collected. The ^{1}H NMRD profiles were recorded at 5°, 15°, 25°, and 35°C on a field cycling relaxometer[32] at NY Medical College over the frequency range 0.01-50 MHz (0.0002 – 1.2 tesla). Each dispersion curve consisted of a total of 22 data points.

O-17 NMR—$H_2{}^{17}O$ transverse relaxation rates were determined for a PBS buffer solution in the presence and absence of ca. 10 mmolal gadolinium complex (exact concentration determined by ICP-MS) as a function of temperature (-5 – 95 °C) on a Varian Unity 300 NMR operating at 40.6 MHz. Probe temperatures were determined from ethylene glycol or methanol chemical shift calibration curves. T_2 was determined by a CPMG pulse sequence

RESULTS

Synthesis

The t-butyl protected, advanced intermediate **16** shown in Figure 2 was synthesized in 48% overall yield over 4 steps. The pentamethyl hydroxybiphenyl **12** was used previously for serum albumin targeting and was known to provide good affinity when linked to a metal complex via a phosphodiester.[28] Phosphoramidite chemistry, similar to what was reported previously[28,33] was used to prepare the phosphodiester **14**. The reaction with (S)-2,5-dihydroxypentanoic acid tert-butyl ester is regiospecific for the primary alcohol. Compound **14** was converted to the nosylate for further reaction with protected 1,7-DO2A. The nosylate provided a good balance of reactivity with shelf stability. We used an excess of DO2A to the nosylate (2:1) to favor alkylation of only one nitrogen, but most of the excess DO2A could be recovered.

This advanced intermediate **16** could then be further alkylated at the N7 position with a range of functional groups denoted $\mathbf{D_1}$ in Figure 2. Regioisomers may be prepared if the 1,4-DO2A is used and one example of a regioisomer with 1,4-substitution was synthesized following a similar synthetic protocol but starting from 1,4-DO2A.[34] Further conversion to the gadolinium complex followed three common steps: acid deprotection of the tert-butyl groups, neutralization, metallation with gadolinium chloride, then preparative HPLC to give the final purified compound. Compounds were assessed for purity by LC-MS and stock solutions then prepared for biophysical studies with accurate gadolinium concentration determined by ICP-MS.

A range of compounds were prepared and analyzed and are shown in Figure 3. A series of alpha-substituted acetates explores whether the size or charge of the substituent influences relaxivity. Two sets of diastereomers **Gd1c/Gd1d** and **Gd1e/Gd1f** were also evaluated to determine if chirality at this center influenced relaxivity. A series of amide donors with

different substituents was prepared to determine how these substituents may affect relaxivity through second sphere effects. Donor atoms based on basic nitrogen heterocycles (e.g. pyridine and imidazole derivatives) were employed. A series of three hydroxyl donors were prepared with 0, 1, or 2 trifluoromethyl groups alpha to the hydroxyl group in order to assess the role of the electron withdrawing CF_3 group on oxygen coordination to gadolinium and subsequent relaxivity. Examples of negatively charged oxygen atom donors (phenolates, hydroxamate, and phosphonate) were screened as was a negatively charged nitrogen atom donor, the methylsulfonamide, which coordinates Gd via the deprotonated nitrogen. Some examples of compounds without a donor atom for Gd in position N7 were prepared (compounds **Gd6a-d**) which were expected to have 2 inner-sphere waters. The effect of having 4 substituted acids was explored (**Gd10a**). Finally the regiochemical isomer of **Gd1c** (**Gd11a**) where 1,4-DO2A was used for the synthesis provided an example of the effect this isomerism may have on relaxivity. Of the compounds listed in Figure 3, three were reported previously: **Gd2a**, **Gd3b** and **Gd6c**.[23,24]

Protein Binding

Binding of the complexes to human serum albumin (HSA) was assessed under standard conditions of 0.1 mM complex, 0.67 mM HSA (4.5% w/v), pH 7.4 50 mM HEPES buffered saline (HBS) at 37 °C by ultrafiltration across a membrane with a 5000 MW cutoff. The initial (total) gadolinium concentration and the gadolinium concentration in the filtrate (unbound) were assessed by ICP-MS. The unbound fraction is simply the ratio of unbound:total, and the protein-bound fraction is one minus this unbound fraction. For all the gadolinium complexes in this study, there was greater than 98% of complex bound to HSA under these conditions. These findings suggest that the dissociation constant for the albumin bound complex, $K_d < 12$ μM for all the compounds studied here. While the various D_1 substituents may alter the albumin affinity, the measurement of full binding isotherms for each compound was beyond the scope of this study.

Relaxivity

Longitudinal proton relaxation rates (R1) were measured in HEPES buffer, pH 7.4, 37 °C at two proton Larmor frequencies, 20 MHz and 60 MHz corresponding to 0.47 and 1.41T, respectively. Measurements were made with gadolinium concentrations ranging from 0 to 0.1 mM and either no HSA or with 0.67 mM HSA. Relaxivity (r_1) was calculated from the slope of the R1 dependence on concentration. Relaxivities in HSA reported are all "observed" relaxivities, i.e. the relaxivity obtained from the R1 dependence and not calculated to reflect the relaxivity of the protein-bound species. However since the fraction bound to HSA is very high under the conditions used (>98%), the observed relaxivity is essentially that of the protein-bound species.

Figure 4a shows the relaxivity of these compounds in HEPES buffer at 1.4T plotted versus molecular weight. As expected, most relaxivities are similar and increase with increasing molecular weight.[35] There are clearly some outliers in Figure 4a and these are denoted by different symbols. **Gd3b** which is contains a pyridyl donor with a carboxylate group *ortho* to the pyridine is known to be $q = 0$ (both the pyridine N and carboxylate O atoms coordinate to Gd) and the relaxivity is low as a result.[24] The compounds **Gd6a-d** have D_1 groups that do not coordinate to Gd(III) and are expected to be $q = 2$ and **Gd6c** was shown previously to be $q = 2$.[24] The additional inner-sphere water would account for the higher relaxivity. Finally there are some compounds like **Gd4a** and **Gd5c** (open circles) that show lower than expected relaxivity but do not appear to be $q = 0$. They may exist as a mixture of $q = 0$ and $q = 1$ species.

Figure 4b shows the relaxivity of these compounds in HSA solution with the relaxivity measured at 0.47T plotted versus that at 1.4T. There is a strong correlation between the two albumin bound relaxivities for all compounds. Interestingly the 4 compounds with the highest relaxivity in the absence of protein (**Gd6a-d**, squares) all have the lowest relaxivity when bound to protein (except for **Gd3b** which is $q = 0$). Previously it was shown that the two inner-sphere water molecules in **Gd6c** were displaced by a protein side chain upon binding to HSA.[24] It is likely that protein side chain from a glutamate or aspartate residue is displacing the inner-sphere water molecules in **Gd6a**, **Gd6b**, and **Gd6d**. Similar effects have been reported for other $q = 2$ complexes non covalently bound to albumin.[36]

Figure 5 shows the relaxivities measured in HSA plotted according to donor type. The highest relaxivities at both fields were seen with the alpha-substituted acetates, Figure 5a. Relaxivities as high as 55.5 $mM^{-1}s^{-1}$ (**Gd1f**) at 0.47T and 32.6 $mM^{-1}s^{-1}$ (**Gd1g**) at 1.4T were observed. There were small differences among the different substitutions. For instance the diasteromeric pairs **Gd1c** and **Gd1d** or **Gd1e** and **Gd1f** showed some difference in relaxivities that were mainly evident at 0.47T. The regioisomers **Gd1c** and **Gd11a** also showed some differences. However as a class, all of these alpha-substituted acetates showed higher relaxivity than the other donor types.

The amide group (Figure 5b) showed lower relaxivities, but there were sharp differences among the amide substituents. For instance going from N-CH_3 (**Gd2a**) to N-CH_2COOH (**Gd2b**) resulted in an increase of 30% in relaxivity, but an additional methylene unit N-CH_2CH_2COOH (**Gd2c**) showed similar relaxivity to the N-CH_3 derivative. The N-methylenephosphonate derivatives (**Gd2f** and **Gd2g**) also showed higher relaxivity relative to the N-methyl suggesting that there may be an additional second-sphere contribution to relaxivity arising from exchangeable hydrogen (waters) with long residency times (>1 ns) in the second coordination sphere. This second-sphere contribution in tetra-substituted amides has been noted before.[37]

Of the nitrogen heterocycles, the best example for relaxivity was the imidazole derivative **Gd3d**. The phenolate donor gave good relaxivity for the *para*-nitro derivative **Gd4c** but rather poor relaxivity for the unsubstituted phenolate **Gd4a** (Figure 5c). The hydroxyl derivatives all showed rather low relaxivity. The alkyl substituted compounds had quite low relaxivity as discussed above and this is likely a result of them being $q = 0$ when bound to protein. Finally the hydroxamate (**Gd7a**), sulfonamide (**Gd8a**), and tetra(alpha-substituted) acid (**Gd10a**) derivatives showed intermediate relaxivity. When D_1 was methylphosphonate, the relaxivity was low.

Nuclear Magnetic Relaxation Dispersion (NMRD)

Nuclear magnetic relaxation dispersion (NMRD) is a measure of longitudinal relaxivity (or relaxation rate) as a function of magnetic field or Larmor frequency. To better understand the differences in relaxivity among these compounds, NMRD profiles of 26 of these compounds (0.1 mM) in HSA solution (0.66 mM, pH 7.4) were recorded each at 4 temperatures: 5, 15, 25, and 35 °C. The HSA solutions alone also show a field dependence on relaxation rate.[32] The NMRD relaxivity was calculated for each magnetic field and temperature using equation 1, and subtracting the appropriate diamagnetic relaxation rate for HSA solution at that same field and temperature.

Examples of NMRD relaxivities in HSA solution are shown in Figure 6a and 6b for compounds **Gd1a** and **Gd3b**, respectively. As discussed above, it is convenient for the purpose of analysis to factor relaxivity into contributions arising from the inner-sphere water and from contributions from second-sphere and outer-sphere water. It was assumed that the contributions to relaxivity arising from second- and outer-sphere water could be estimated

from the relaxivity of **Gd3b** in HSA, since it contains no inner-sphere water. The relaxivity of **Gd3b** then was subtracted from the relaxivity of each compound at the corresponding temperature and field strength. As an example, Figure 6c shows this difference for **Gd1a**, which reflects the inner-sphere contribution to relaxivity for **Gd1a**. The inner-sphere relaxivity of **Gd1a** decreases with decreasing temperature. This indicates that the system is in slow exchange ($T_{1m} < \tau_m$) and that analysis of this data should provide an accurate estimate of the water residency time τ_m.

The variable temperature NMRD data was analyzed as follows. First, the higher field NMRD data only were considered ($\nu_H \geq 6$ MHz). At these fields, the contribution to electronic relaxation from the static zero-field splitting (ZFS) is negligible and use of modified Solomon-Bloembergen-Morgan theory is appropriate.[38,39] We found it necessary to apply the Lipari-Szabo modification of the spectral density term to account for internal motion.[40] At these proton frequencies (6 MHz and up), the contribution to relaxation dependent on the electronic Larmor frequency, ω_s, has dispersed and the relaxation of the inner-sphere water is given by equation 6

$$\frac{1}{T_{1m}} = \frac{2}{15}\left(\frac{\mu_0}{4\pi}\right)\frac{\gamma_H^2 g_e^2 \mu_B^2 S(S+1)}{r_{GdH}^6}\left[\frac{3F^2\tau_c}{1+\omega_H^2\tau_c^2} + \frac{3\left(1-F^2\right)\tau_f}{1+\omega_H^2\tau_f^2}\right] \quad (6)$$

where τ_f is a correlation time that takes into account fast local motion ($1/\tau_f = 1/\tau_c + 1/\tau_l$) and τ_l is a correlation time for fast motion; F^2 is an order parameter (often denoted S^2, but here F is used to avoid confusion with the spin quantum number). ω_H is the Larmor frequency of the proton (rad/s), γ_H is the proton magnetogyric ratio, g_e is the electronic g-factor ($g_e = 2$ for Gd(III)), μ_B is the Bohr magneton, and μ_0 is the permittivity of vacuum. The field dependence on T_{1e} is given by equation 7.

$$\frac{1}{T_{1e}} = \frac{\Delta_t^2\left[4S(S+1)-3\right]}{25}\left[\frac{\tau_v}{1+\omega_s^2\tau_v^2} + \frac{4\tau_v}{1+4\omega_s^2\tau_v^2}\right] \quad (7)$$

The various correlation times should all be temperature dependent, however we found that because rotation is already slow because of protein binding and did not limit relaxivity, the data could be well fit with a single, temperature independent τ_R (i.e. the temperature dependence on τ_R was not well defined). Similarly it is known from previous work that τ_v has a weak temperature dependence[11,21] and we found that all the variable temperature NMRD data could be well fit with a single τ_v. We also found that the data was insensitive to the fast internal motion correlation time τ_l, which was always very short (≤100 ps). Under these conditions the $(1\text{-}F^2)\tau_f/(1+\omega_H^2\tau_f^2)$ term tends to zero and introducing a term for the temperature dependence of τ_l is meaningless. The data are however very sensitive to τ_m and its temperature dependence is given by equation 8 where τ_m^{310}[10] is the water residency time at 37 °C and $\Delta H^{\ddagger}$ is the activation energy for water exchange.

$$\frac{1}{\tau_m} = k_{ex} = \frac{T}{310.15\tau_m^{310}}\left[\frac{\Delta H^{\square}}{R}\left(\frac{1}{T} - \frac{1}{310.15}\right)\right] \quad (8)$$

Altogether the variable temperature NMRD data (4 temperatures, 60 data points) could be well fit using 6 parameters: τ_R, τ_v, τ_m^{310}, $\Delta H^{\ddagger}$, Δ^2, and F^2. NMRD data for each compound was simultaneously fit to equations 2, 6, 7, and 8 with the relaxivity of **Gd3b** assumed to be equal to the contribution to relaxivity from second/outer-sphere water. Examples of the

observed NMRD relaxivities and the fitted data are shown in Figure 7. Figure 7 shows the range of behaviors encountered. Figure 7A shows relaxivity of **Gd4b** (phenolate donor) where the relaxivity is increasing as temperature decreases. This indicates that the system is in fast exchange ($T_{1m} > \tau_m$). At 5 °C very high relaxivities were observed with this compound but at 35 °C, relaxivity appears limited by water exchange that is too fast. Figure 7B shows data for the alpha-substituted (isopropyl) acetate derivative **Gd1c**. Here relaxivity is high and practically independent of temperature. Recall from Fig 6B that the second/outer-sphere relaxivity is increasing as temperature decreases, and so the inner-sphere component must actually decrease slightly with decreasing temperature. Figure 7C shows data for the hydroxamate derivative **Gd7a**. The relaxivities are lower and the highest relaxivities are observed at 35 °C. This suggests this system is limited by slow water exchange, since as the temperature is lowered τ_m will increase and dominate the ($T_{1m} + \tau_m$) term. Figure 7D shows NMRD data for the amide derivative **Gd2c**. This is one of the lowest relaxivities observed and again, the relaxivity decreases with decreasing temperature, suggesting relaxivity limited by slow water exchange. The very flat NMRD profile at lower temperatures is also typical of a system dominated by very slow exchange.

In total, NMRD data for 25 compounds was analyzed. The results of these six parameter NMRD analyses are given in Table 1 along with the estimated standard deviation for each parameter in parentheses. The water residency time at 37 °C (τ_m^{310}) ranged from 0.7 to 612 ns, or over three orders of magnitude. In Table 1 the mean parameter values for all 25 compounds are listed along with relative standard deviations (RSD). There is wide variability in the water residency times, but much less variation among the other parameters. The values of τ_R are in the range reported for other complexes non-covalently bound to serum albumin.[21,41,42] It was necessary to use the Lipari-Szabo approach, although the correlation time for fast motion could not be determined accurately and only an upper limit of 0.1 ns could be given. The values of τ_v are also similar to reported numbers for these types of gadolinium complexes.[11,43,44] The Δ^2 numbers are much smaller by a factor of 3-5 than what is typically reported for fast tumbling GdDOTA derivatives, i.e. electronic relaxation of the protein bound compounds is slower than may have been anticipated from the literature. This inconsistency may arise from the use of approximate theories for the relaxivity of small complexes where the effect of the static ZFS is neglected. It has been shown that when the fast rotational motion is included as source of modulation of static ZFS, smaller Δ^2 values are always obtained.[22] Furthermore, more thorough analyses of multifrequency EPR and NMRD of $[Gd(DOTA)(H_2O)]^{2-}$ which take static ZFS into account show lower values of Δ^2.[16,17,45]

The most uncertainty in the fitted parameters arose for compounds where water exchange was either very fast or very slow. In the former case, the short residency time τ_m is the dominant correlation time for relaxation (see equation 4). As a result, the NMRD profile is less sensitive to the slow rotational correlation time and τ_R is less well defined. On the other extreme, when water exchange is very slow ($\tau_m > T_{1m}$), the NMRD profile is not very sensitive to the relaxation time of the bound water molecule (T_{1m}) and as a result τ_R, τ_v, and Δ^2 are less well defined. Nonetheless the fact that similar τ_R values are obtained among all 25 compounds appears to validate the use of a common albumin-binding group to immobilize these complexes.

Oxygen-17 relaxometry

Typically water exchange rates at gadolinium complexes are estimated from the temperature dependence of the O-17 transverse relaxation rate of bulk water in the presence and absence of the complex. The O-17 technique is generally not sensitive enough to measure water exchange of protein-bound complexes. This is because of solubility limitations of the protein and also because the baseline relaxation rate of water in concentrated protein solution is

already quite high. Although it has been shown that protein-binding can alter the water exchange rate of the complex,[20] a series of O-17 studies was performed without HSA to determine if the same general trends in water exchange rate were seen in the absence of protein.

The data treatment has been amply described previously.[21] For Gd^{3+} complexes, where the paramagnetic chemical shift of the bound water is small compared to its transverse relaxation time, the so-called reduced relaxation rate ($1/T_{2r}$) is given by equation 9, where R_{2p} and R_{2d} are the relaxation rates measured in the presence and absence of gadolinium complex, respectively.

$$\frac{1}{T_{2r}} = \frac{\left(R_{2p} - R_{2d}\right)}{(q/[H_2O])} = \frac{1}{T_{2m} + \tau_m} \tag{9}$$

At low temperatures where the slow exchange limit ($\tau_m >> T_{2m}$) is reached, the reduced relaxation rate becomes the water exchange rate, i.e. $1/T_{2r} = 1/\tau_m$. Figure 8 shows variable temperature O-17 data for 6 compounds where the water exchange rate is increasing from Figure 8A through 8F. The maximum (where $\tau_m = T_{2m}$) moves increasingly to lower temperatures from Fig 8A through to 8F, and if one inspects the low temperature limit (right side, slow exchange limit) of each graph, it is obvious that the water exchange rate is increasing through this series. The donor atom series in Figure 8 from A to F is pyridyl, amide, hydroxamate, acetate, substituted acetate, and then **Gd10a**, which has 4 substituted acetate donors. The water exchange parameters are listed in Table 2 and are in reasonable agreement with those estimated for the protein-bound complexes.

DISCUSSION

The overall approach to identifying high relaxivity compounds appears justified. The derivatives where the D_1 group was an alpha-substituted acetate gave the highest relaxivities at both fields. Relaxivities in the 45 – 55 $mM^{-1}s^{-1}$ range at 0.47T and 26 – 32 $mM^{-1}s^{-1}$ at 1.4T were observed with this group. Other donor atom substitutions either made water exchange too fast or too slow. In Figure 9A the measured relaxivities at both fields are plotted versus τ_m values obtained from the NMRD fits. The observed behavior is exactly as predicted by theory wherein there is an optimal range for τ_m with respect to relaxivity. The solid lines in Figure 9A were generated from the average values for the rotational and electronic relaxation parameters in Table 1. Although it is likely that each compound has slightly different rotational dynamics, the reasonably good agreement of this composite curve in Figure 9A with the data validates the overall approach of screening compounds with a common albumin binding group. Figure 9A also experimentally demonstrates that the optimal water exchange regime is much smaller at 0.47T than it is at 1.4T. Optimization of water exchange is clearly much more important at low fields. This point has been made previously based on simulations,[8,46] and this study provides experimental data to support those simulations. Note also that at 1.4T the optimum value for water residency time is shifted compared to 0.47T.

Figure 9B shows the correlation between the electronic relaxation parameter Δ^2 and measured relaxivity. There is a good negative correlation (r = -0.69 for both fields) between relaxivity and Δ^2. This may be expected since as Δ^2 becomes smaller, T_{1e} becomes longer. At low fields T_{1e} is, or contributes significantly to the overall correlation time, see equation 4. Increasing T_{1e} will increase relaxivity. However T_{1e} will increase with the square of the applied field (eq 7), so at high fields, the contribution of T_{1e} to the overall correlation time τ_c becomes smaller, and the importance of Δ^2 on relaxivity decreases with increasing field.

This is apparent in Figure 9B where the slope of correlation line at low field (0.47T) is twice as great as at 1.4T.

The magnitude of Δ^2 determined in this study is smaller by a factor of 3 to 4 compared with values reported for DOTA derivatives, which were not bound to proteins.[11,44] For slow tumbling compounds Δ^2 strongly influences where the peak in the NMRD curve will occur. The values of Δ^2 in the literature would predict a relaxivity maximum occurring between 0.8 – 0.9T (35 – 40 MHz) while we typically observed maxima at ca. 0.5T.

Other parameters such as τ_v and the order parameter F^2 did not correlate with relaxivity. τ_v is the correlation time for modulation of the transient zero field splitting. The origin of this picosecond correlation time is believed to be either from vibrational modes of the metal complex or solvent collisions. Since the complexes are all very similar in structure as DOTA derivatives, one may expect similar vibrational energies; similarly the rate of solvent collisions should not differ among the different complexes. Differences in the order parameter may simply be due to differences in internal motion. For instance, the donor group may also interact with the protein and serve to rigidify the chelate:protein complex and reduce internal motion. Another possibility is differences in second-sphere relaxivity among the compounds. Mathematically, the order parameter F^2 scales the spectral density function. If some compounds had higher or lower second-sphere relaxivity than that of the $q = 0$ compound **Gd3b** then the order parameter would have been higher or lower, respectively, in order to compensate.

Overall the relaxivities are not as high as predicted by theory. This is certainly a result of internal motion. The rotational correlation times estimated from NMRD are shorter than those anticipated for a protein the size of albumin. This phenomenon has been seen before and the reduced τ_R values likely reflect internal motion along the bonds from the biphenyl binding group to the metal complex. It is also known that the coordinated water itself undergoes rotation and this will further serve to limit relaxivity.[47,48] Reducing internal motion should lead to higher relaxivities. Consider **Gd4b** whose water exchange rate was too fast at 37 °C. At lower temperatures, the exchange rate for this compound enters the optimal range; at the same time, all motion is slowing down as the temperature is lowered. Relaxivities as high as 71 $mM^{-1}s^{-1}$ were observed for **Gd4b** at 5 °C and this demonstrates the potential low field relaxivities that may be obtained.

Structure – Activity Relationships

In general, the effect of donor group on water exchange rate was in accord with what has been reported in the literature. Donor groups increased water exchange rate in the order: phosphonate ~ phenolate > α-substituted acetate > acetate > hydroxamate ~ sulfonamide > amide ~ pyridyl ~ imidazole. There are examples of DOTA derivatives with a single phosphonate,[44] phenolate,[49] α-substituted acetate,[50] sulfonamide,[51] amide,[11,52] and pyridyl[53] substitution, and in the cases where water exchange data were reported,[18] the values are in a similar range to what is observed here. The hydroxamate donor and some of the N-heterocycles had not been reported to our knowledge. Replacing an acetate with a neutral donor slowed down water exchange in all cases and resulted in lower relaxivity. The phosphonate and phenolate substitutions increased water exchange to the point that fast water exchange limited relaxivity. It is known that sequential replacement of acetate groups by phosphonate groups will eventually lead to a reduction in coordination number from 9 to 8 and there will no longer be a coordinated water. In the case of the single phosphonate substitution it may be that the 8-coordinate transition state is sufficiently stabilized to lead to facile water exchange via a dissociative mechanism, and a very fast exchange rate was also reported for a related phosphonate derivative.[44]

Among the alpha-substituted acetates, we compared the effect of chirality on relaxivity and its molecular determinants. **Gd1c**/**Gd1d** and **Gd1e**/**Gd1f** are both diastereomeric pairs with *R*- and *S*-substituted acetates, respectively. In all the compounds the protein binding group is branched from an acetate with *R* configuration. Thus **Gd1c** is an *R,R* diastereomer and **Gd1d** is an *R,S* diasteromer. In both cases the *R,R* diastereomers showed 3-4 fold faster water exchange than the corresponding *R,S* analog. However differences in relaxivity among these compounds were minor since the exchange rates were all within the optimal range. Similarly the regioisomers **Gd1c** and **Gd11a** differed by the placement of the substituted acetate. The former was on N7 while the latter was substituted at N4. Again, small differences in water exchange rate were observed but relaxivities were similar. It is well established that DOTA derivatives can adopt two conformational isomers: square antiprism (SAP) where, looking down the water oxygen to gadolinium bond, the 4 nitrogens form one square and the 4 acetate oxygens form another square that is staggered 45° from the nitrogen containing square; and a twisted square antiprism (TSAP) where this angle is reduced.[54,55] The TSAP isomers usually have faster water exchange kinetics. The distribution between SAP and TSAP isomerism was not investigated in this study, but it may be behind the differences in water exchange rate observed in the various alpha-substituted acetates where τ_m^{310} ranged from 10 to 75 ns. Increasing the number of alpha-substituted acetates is known to increase the water exchange rate,[54-56] and a similar effect was observed here with **Gd10a** where τ_m^{310} was only 2 ns.

For the neutral donors where water exchange was slow it is not possible to definitively rank these donor groups in terms of effect on water exchange because the uncertainty in τ_m for these compounds is of the same order as the differences among them. Similarly, the effect of a phenolate or phosphonate donor on water exchange appears comparable.

There are clear trends in terms of the electronic relaxation parameter Δ^2. It seems that this is related to symmetry. The lowest value of Δ^2 (longest T_{1e}) was found with the unsubstituted acetate, where the ligand field created by the 4 cyclen N, 4 carboxylate O, and water O donors would have apparent C_{4v} symmetry. The substituted acetates all showed the next lowest values of Δ^2, likely due to the all acetate donor set. The next tier could be defined as non-acetate oxygen donor atoms (amide, phenolate, etc). The compounds with the largest value of Δ^2 were those with a neutral nitrogen donor atom.

This study did not explicity address second-sphere contributions to relaxivity. It is known that exchangeable hydrogen atoms in the second sphere, either from waters of hydration or protonated acids, can make significant contributions to relaxivity. For instance an albumin-bound complex with no inner-sphere water was reported to have relaxivities greater than 20 $mM^{-1}s^{-1}$ at 0.47T.[57] Among the amide series in this study (**Gd2a-g**), we noted higher than expected relaxivity for the amide derived from glycine (**Gd2b**). Its relaxivity was 30% higher compared to **Gd2a** which had no pendant carboxylate groups. The relaxivity of **Gd2b** was also significantly higher than **Gd2c** or **Gd2d** which had pendant carboxylates but also additional methylene units. Higher relaxivity was also noted for the methylenephosphonate derivatives **Gd2f** and **Gd2g**. Indeed the tetra-amide compound, where each amide has a methylenephosphonate group shows high, pH-dependent relaxivity even though the inner-sphere water is undergoing extremely slow water exchange.[37,58,59] The high relaxivity of these tetraamides must be attributed to second-sphere effects.

Utilizing amide substituents to organize the second hydration sphere would seem a useful strategy to increase relaxivity further. Unfortunately, amide donors have a negative effect on inner-sphere water exchange rate in terms of gadolinium relaxivity. In a subsequent paper, we will explore the potential of using amide substituents to increase second-sphere

relaxivity while varying the other donor groups to optimize the inner-sphere water exchange rate and in turn, inner-sphere relaxivity.[60]

CONCLUSION

Overall this study demonstrates that the water exchange rate at GdDOTA derivatives can be exquisitely tailored over 3 orders of magnitude by the choice of donor atom. Donor atom choice has a predictable effect on electronic relaxation as well through the parameter Δ^2. For protein bound complexes this results in a range of relaxivities where the alpha-substituted acetate was the preferred donor group. Other donor groups resulted in relaxivity that was limited by too fast a water exchange rate (e.g. phenolate or phosphonate donor groups) or too slow a water exchange rate (e.g. amide or pyridyl). Differences among compounds with the same donor atom may be ascribed to differences in second-sphere relaxivity and this avenue may be explored for further gains in relaxivity. However, even with an optimal water exchange rate, relaxivities observed in this study were still limited by fast internal motions.

Acknowledgments

PC acknowledges financial support from the National Institutes of Health through grants R01EB009062 and R21EB009738.

REFERENCES

1. Grobner T, Prischl FC. Gadolinium and nephrogenic systemic fibrosis. Kidney Int 2007;72:260–264. [PubMed: 17507905]
2. Rydahl C, Thomsen HS, Marckmann P. High Prevalence of Nephrogenic Systemic Fibrosis in Chronic Renal Failure Patients Exposed to Gadodiamide, a Gadolinium-Containing Magnetic Resonance Contrast Agent. Invest Radiol 2008;43:141–144. [PubMed: 18197066]
3. Haylor J, Dencausse A, Vickers M, et al. Nephrogenic Gadolinium Biodistribution and Skin Cellularity Following a Single Injection of Omniscan in the Rat. Invest Radiol 2010;45:XXX–XXX.
4. Aime S, Castelli DD, Crich SG, et al. Pushing the sensitivity envelope of lanthanide-based magnetic resonance imaging (MRI) contrast agents for molecular imaging applications. Acc Chem Res 2009;42:822–831. [PubMed: 19534516]
5. Major JL, Meade TJ. Bioresponsive, cell-penetrating, and multimeric MR contrast agents. Acc Chem Res 2009;42:893–903. [PubMed: 19537782]
6. Datta A, Raymond KN. Gd-hydroxypyridinone (HOPO)-based high-relaxivity magnetic resonance imaging (MRI) contrast agents. Acc Chem Res 2009;42:938–947. [PubMed: 19505089]
7. Bazeli R, Coutard M, Daumas-Duport B, et al. In Vivo Evaluation of a New MRI Contrast Agent (P947) to Target Matrix Metalloproteinases in Expanding Experimental Abdominal Aortic Aneurysms. Invest Radiol 2010;45:XXX–XXX.
8. Caravan P. Strategies for increasing the sensitivity of gadolinium based MRI contrast agents. Chem Soc Rev 2006;35:512–523. [PubMed: 16729145]
9. Caravan P, Ellison JJ, McMurry TJ, et al. Gadolinium(III) Chelates as MRI Contrast Agents: Structure, Dynamics, and Applications. Chem Rev 1999;99:2293–2352. [PubMed: 11749483]
10. Laurent S, Elst LV, Muller RN. Comparative study of the physicochemical properties of six clinical low molecular weight gadolinium contrast agents. Contrast Media Mol Imaging 2006;1:128–137. [PubMed: 17193689]
11. Powell DH, Ni Dhubhghaill OM, Pubanz D, et al. Structural and Dynamic Parameters Obtained from 17O NMR, EPR, and NMRD Studies of Monomeric and Dimeric Gd3+ Complexes of Interest in Magnetic Resonance Imaging: An Integrated and Theoretically Self-Consistent Approach. J Am Chem Soc 1996;118:9333–9346.
12. Caravan P, Astashkin AV, Raitsimring AM. The gadolinium(III)-water hydrogen distance in MRI contrast agents. Inorg Chem 2003;42:3972–3974. [PubMed: 12817950]

13. Raitsimring AM, Astashkin AV, Poluektov OG, et al. High field pulsed EPR and ENDOR of Gd^{3+} complexes in glassy solutions. Appl Magn Reson 2005;28:281–295.
14. Astashkin AV, Raitsimring AM, Caravan P. Pulsed ENDOR Study of Water Coordination to Gd3+ Complexes in Orientationally Disordered Systems. J Phys Chem A 2004;108:1900–2001.
15. Lauffer RB. Targeted Relaxation Enhancement Agents for MRI. Magn Reson Med 1991;22:339. [PubMed: 1812368]
16. Benmelouka M, Van Tol J, Borel A, et al. A high-frequency EPR study of frozen solutions of Gd(III) complexes: straightforward determination of the zero-field splitting parameters and simulation of the NMRD profiles. J Am Chem Soc 2006;128:7807–7816. [PubMed: 16771494]
17. Borel A, Helm L, Merbach AE, et al. T1e in Four Gd3+ Chelates: LODEPR Measurements and Models for Electron Spin Relaxation. J Phys Chem A 2002;106:6229–6231.
18. Helm L, Merbach AE. Inorganic and bioinorganic solvent exchange mechanisms. Chem Rev 2005;105:1923–1959. [PubMed: 15941206]
19. Eldredge HB, Spiller M, Chasse JM, et al. Species dependence on plasma protein binding and relaxivity of the gadolinium-based MRI contrast agent MS-325. Invest Radiol 2006;41:229–243. [PubMed: 16481905]
20. Zech SG, Eldredge HB, Lowe MP, et al. Protein binding to lanthanide(III) complexes can reduce the water exchange rate at the lanthanide. Inorg Chem 2007;46:3576–3584. [PubMed: 17425306]
21. Caravan P, Parigi G, Chasse JM, et al. Albumin Binding, Relaxivity, and Water Exchange Kinetics of the Diastereoisomers of MS-325, a Gadolinium(III)-Based Magnetic Resonance Angiography Contrast Agent. Inorg Chem 2007;46:6632–6639. [PubMed: 17625839]
22. Kruk D, Kowalewski J. Nuclear spin relaxation in paramagnetic systems (S≥1) under fast rotation conditions. J Magn Reson 2003;162:229–240. [PubMed: 12810007]
23. Raitsimring AM, Astashkin AV, Baute D, et al. Determination of the hydration number of gadolinium(III) complexes by high-field pulsed (17)O ENDOR spectroscopy. ChemPhysChem 2006;7:1590–1597. [PubMed: 16810729]
24. Zech S, Sun W-C, Jacques V, et al. Probing the Water Coordination of Protein-Targeted MRI Contrast Agents by Pulsed ENDOR Spectroscopy. ChemPhysChem 2005;6:2570–2577. [PubMed: 16294353]
25. Caravan, P.; Jacques, V.; Dumas, S., et al. Synthesis of high relaxivity chelates for potential use as MRI contrast agents.. 2008. PCT WO2008098056
26. Bannwarth W, Kung E. Bis(allyloxy)(diisopropylamino)phosphine as a new phosphinylation reagent for the phosphorylation of hydroxy functions. Tetrahedron Lett 1989;30:4219–4222.
27. Bannwarth W, Trzeciak A. A Simple and Effective Chemical Phosphorylation Procedure for Biomolecules. Helv Chim Acta 1987;70:175–186.
28. Dumas S, Troughton JS, Cloutier NJ, et al. A High Relaxivity Magnetic Resonance Imaging Contrast Agent Targeted to Serum Albumin. Aus J Chem 2008;61:682–686.
29. Barone AD, Tang JY, Caruthers MH. In situ activation of bis-dialkylaminophosphines--a new method for synthesizing deoxyoligonucleotides on polymer supports. Nucleic Acids Res 1984;12:4051–4061. [PubMed: 6728676]
30. Eguchi C, Kakuta A. The Novel Synthesis of L-Hydroxyproline from D-Glutamic Acid. Bull Chem Soc Japan 1974;47:1704–1708.
31. Schmidt U, Braun C, Sutoris H. Enantioselective Syntheses of (R)- and (S)-Hexahydropyridazine-3-carboxylic Acid Derivatives. Synthesis 1996:223–229.
32. Koenig SH, Brown RD III. Field-cycling relaxometry of protein solutions and tissue: immplications for MRI. Prog Nucl Magn Reson Spectrosc 1990;22:487–567.
33. McMurry TJ, Parmelee DJ, Sajiki H, et al. The effect of a phosphodiester linking group on albumin binding, blood half-life, and relaxivity of intravascular diethylenetriaminepentaacetato aquo gadolinium(III) MRI contrast agents. J Med Chem 2002;45:3465–3474. [PubMed: 12139457]
34. Li C, Wong WT. A simple, regioselective synthesis of 1,4-bis(tert-butoxycarbonylmethyl)-tetraazacyclododecane. J Org Chem 2003;68:2956–2959. [PubMed: 12662076]
35. Ranganathan RS, Fernandez ME, Kang SI, et al. New multimeric magnetic resonance imaging agents. Invest Radiol 1998;33:779–797. [PubMed: 9818313]

36. Aime S, Gianolio E, Terreno E, et al. Ternary Gd(III)L-HSA adducts: evidence for the replacement of inner-sphere water molecules by coordinating groups of the protein. Implications for the design of contrast agents for MRI. J Biol Inorg Chem 2000;5:488–497. [PubMed: 10968620]
37. Kalman FK, Woods M, Caravan P, et al. Potentiometric and relaxometric properties of a gadolinium-based MRI contrast agent for sensing tissue pH. Inorg Chem 2007;46:5260–5270. [PubMed: 17539632]
38. Bloembergen N, Morgan LO. Proton Relaxation Times in Paramagnetic Solutions. Effects of Electron Spin Relaxation. J Chem Phys 1961;34:842–850.
39. Solomon I. Relaxation Processes in a System of Two Spins. Phys Rev 1955;99:559–565.
40. Lipari G, Szabo A. Model-free approach to the interpretation of nuclear magnetic resonance relaxation in macromolecules. 1. Theory and range of validity. J Am Chem Soc 1982;104:4546–4559.
41. Caravan P, Cloutier NJ, Greenfield MT, et al. The interaction of MS-325 with human serum albumin and its effect on proton relaxation rates. J Am Chem Soc 2002;124:3152–3162. [PubMed: 11902904]
42. Troughton JS, Greenfield MT, Greenwood JM, et al. Synthesis and evaluation of a high relaxivity manganese(II)-based MRI contrast agent. Inorg Chem 2004;43:6313–6323. [PubMed: 15446878]
43. Lebduskova P, Hermann P, Helm L, et al. Gadolinium(III) complexes of mono- and diethyl esters of monophosphonic acid analogue of DOTA as potential MRI contrast agents: solution structures and relaxometric studies. Dalton Trans 2007:493–501. [PubMed: 17213936]
44. Rudovsky J, Cigler P, Kotek J, et al. Lanthanide(III) complexes of a mono(methylphosphonate) analogue of H4dota: The influence of protonation of the phosphonate moiety on the TSAP/SAP isomer ratio and the water exchange rate. Chem Eur J 2005;11:2373–2384.
45. Rast S, Fries PH, Belorizky E, et al. A general approach to the electronic spin relaxation of Gd(III) complexes in solutions. Monte Carlo simulations beyond the Redfield limit. Journal of Chemical Physics 2001;115:7554–7563.
46. Caravan P, Farrar CT, Frullano L, et al. Influence of molecular parameters and increasing magnetic field strength on relaxivity of gadolinium- and manganese-based T(1) contrast agents. Contrast Media Mol Imaging 2009;4:89–100. [PubMed: 19177472]
47. Dunand FA, Borel A, Merbach AE. How does internal motion influence the relaxation of the water protons in Ln(III)DOTA-like complexes? J Am Chem Soc 2002;124:710–716. [PubMed: 11804502]
48. Yerly F, Borel A, Helm L, et al. MD simulations of acyclic and macrocyclic Gd3+-based MRI contrast agents: Influence of the internal mobility on water proton relaxivity. Chem Eur J 2003;9:5468–5480.
49. Woods M, Kiefer GE, Bott S, et al. Synthesis, relaxometric and photophysical properties of a new pH-responsive MRI contrast agent: the effect of other ligating groups on dissociation of a pnitrophenolic pendant arm. J Am Chem Soc 2004;126:9248–9256. [PubMed: 15281814]
50. Andre JP, Toth E, Fischer H, et al. High relaxivity for monomeric Gd(DOTA)-based MRI contrast agents, thanks to micellar self-organization. Chem Eur J 1999;5:2977–2983.
51. Lowe MP, Parker D, Reany O, et al. pH-dependent modulation of relaxivity and luminescence in macrocyclic gadolinium and europium complexes based on reversible intramolecular sulfonamide ligation. J Am Chem Soc 2001;123:7601–7609. [PubMed: 11480981]
52. Nicolle GM, Toth E, Schmitt-Willich H, et al. The impact of rigidity and water exchange on the relaxivity of a dendritic MRI contrast agent. Chem Eur J 2002;8:1040–1048.
53. Aime S, Batsanov AS, Botta M, et al. Structure and relaxivity of macrocyclic gadolinium complexes incorporating pyridyl and 4-morpholinopyridyl substituents. New J Chem 1999;23:669–670.
54. Woods M, Aime S, Botta M, et al. Correlation of Water Exchange Rate with Isomeric Composition in Diastereoisomeric Gadolinium Complexes of Tetra(carboxyethyl)dota and Related Macrocyclic Ligands. J Am Chem Soc 2000;122:9781–9792.
55. Woods M, Botta M, Avedano S, et al. Towards the rational design of MRI contrast agents: a practical approach to the synthesis of gadolinium complexes that exhibit optimal water exchange. Dalton Trans 2005:3829–3837. [PubMed: 16311635]

56. Woods M, Kovacs Z, Zhang S, et al. Towards the rational design of magnetic resonance imaging contrast agents: isolation of the two coordination isomers of lanthanide DOTA-type complexes. Angew Chem Int Ed Engl 2003;42:5889–5892. [PubMed: 14673928]

57. Caravan P, Greenfield MT, Li X, et al. The Gd(3+) complex of a fatty acid analogue of DOTP binds to multiple albumin sites with variable water relaxivities. Inorg Chem 2001;40:6580–6587. [PubMed: 11735466]

58. Ali MM, Woods M, Caravan P, et al. Synthesis and relaxometric studies of a dendrimer-based pH-responsive MRI contrast agent. Chem Eur J 2008;14:7250–7258.

59. Woods M, Caravan P, Geraldes CF, et al. The effect of the amide substituent on the biodistribution and tolerance of lanthanide(III) DOTA-tetraamide derivatives. Invest Radiol 2008;43:861–870. [PubMed: 19002058]

60. Jacques V, Dumas S, Sun W-C, et al. High relaxivity MRI contrast agents part 2: Optimization of inner- and Second-sphere Relaxivity. Invest Radiol 2010;45:XXX–XXX.

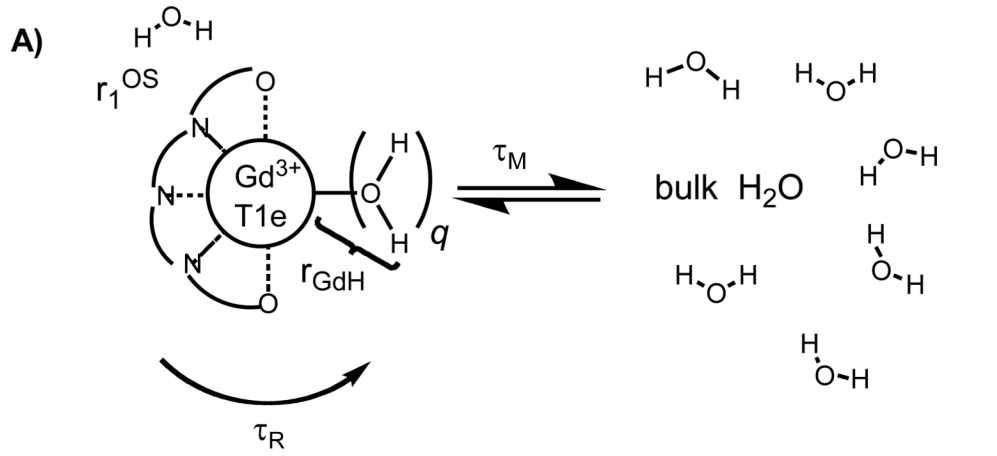

Figure 1.

A) Relaxivity of gadolinium complexes depends on a range of intrinsic molecular factors. B) For fast tumbling complexes, relaxivity is limited by fast rotation and it is not possible to determine how much relaxivity will be increased if rotation were slowed, e.g. by protein binding. C) Relaxivity is increased when the complex is immobilized by binding to a large protein, but other factors may now limit relaxivity.

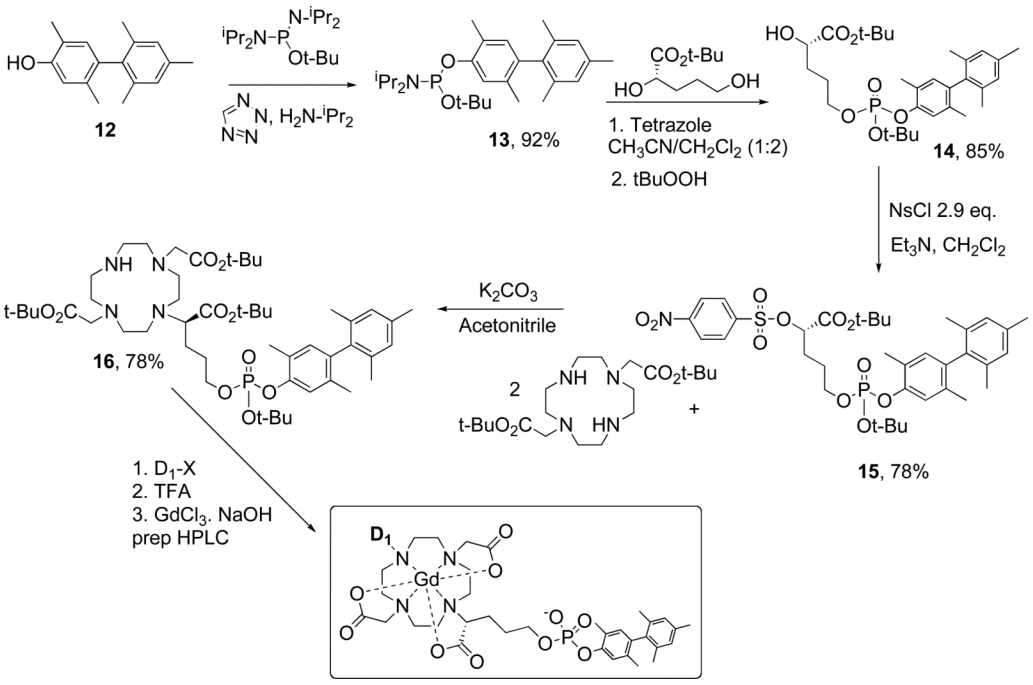

Figure 2.
General synthetic scheme for the compounds described in this report.

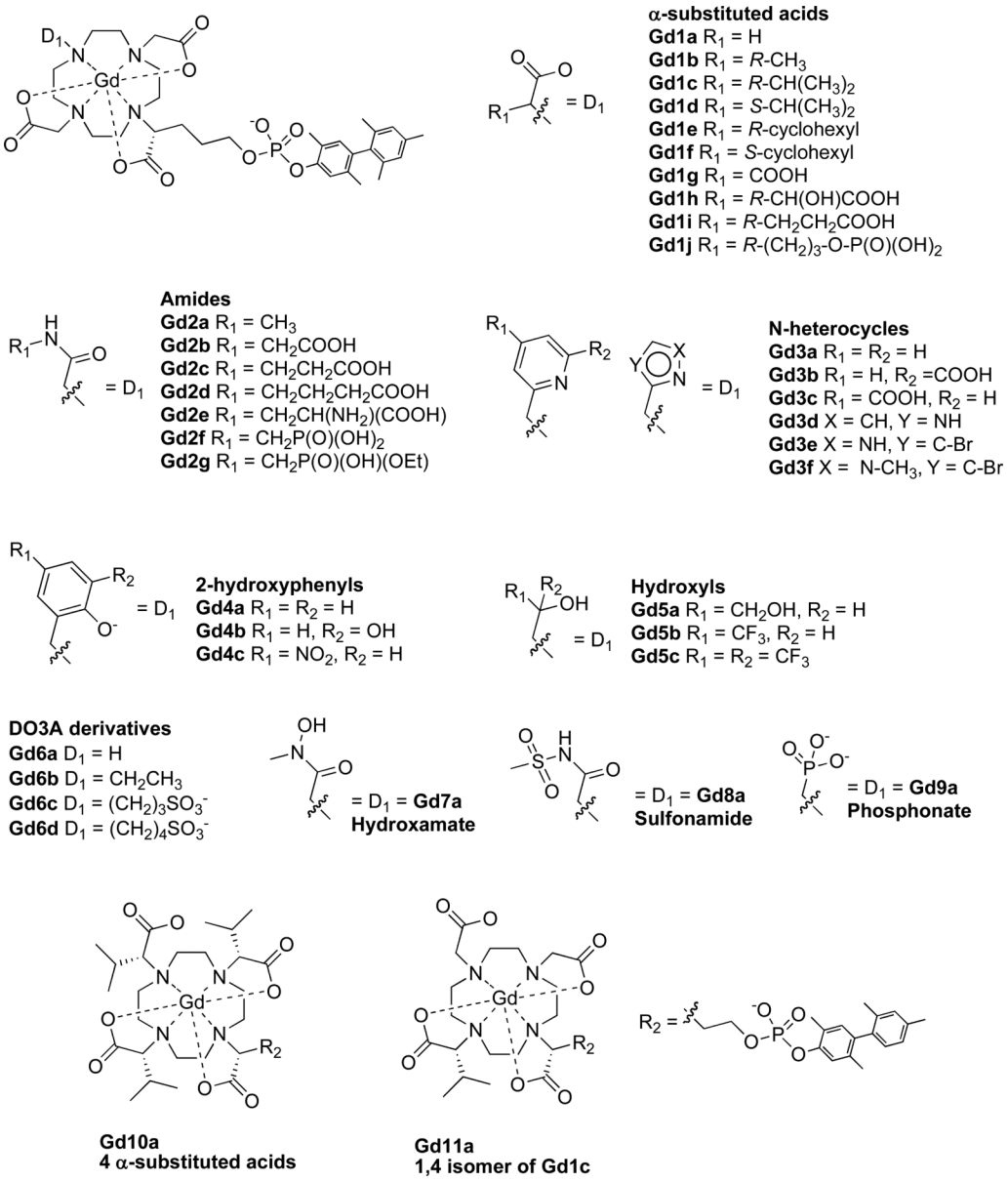

Figure 3.

Chemical structures of the compounds studied in this report arranged by different donor groups.

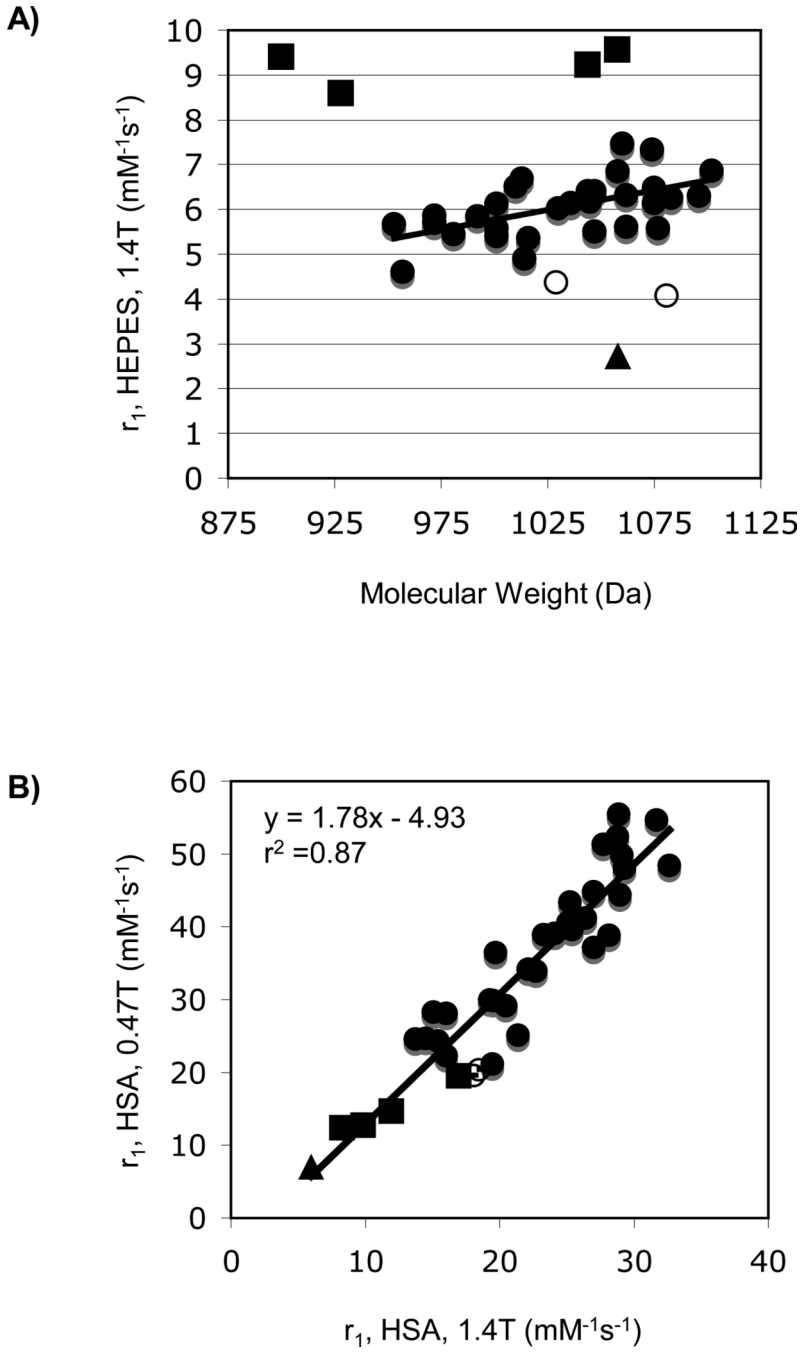

Figure 4.

A) Relaxivities determined in HEPES buffer, pH 7.4, 37 °C at 1.4T plotted versus compound molecular weight. B) Relaxivities determined in HSA solution at 37 °C showing the correlation between r_1 at 0.47T (y-axis) and 1.4T (x-axis). Squares represent suspected q = 2 compounds **Gd6a-d**; triangle is known q = 0 compound **Gd3b**; open circles are outliers **Gd4a** and **Gd5c**.

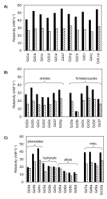

Figure 5.
Relaxivities determined in HSA solution (0.1 mM Gd, 0.67 mM HSA) at 37 °C at 0.47T (black bars) and 1.4T (grey bars). A) Alpha-substituted acetate donors; B) Amide and N-heterocycle donors; C) all other donor groups.

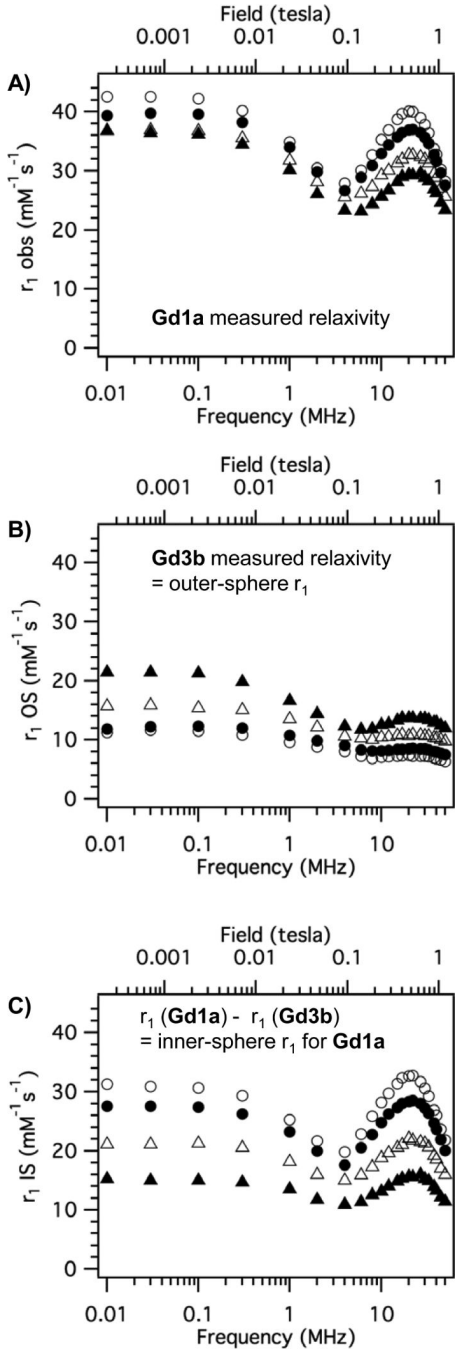

Figure 6.

A) Variable temperature NMRD profile for **Gd1a** in HSA solution. B) Variable temperature NMRD for *q* = 0 complex **Gd3b** in HSA solution. C) Estimated inner-sphere relaxivity of **Gd1a** obtained by subtracting each curve in B from corresponding curve in A. t = 35 °C (open circles); t = 25 °C (filled circles); t = 15 °C (open triangles); t = 5 °C (filled triangles).

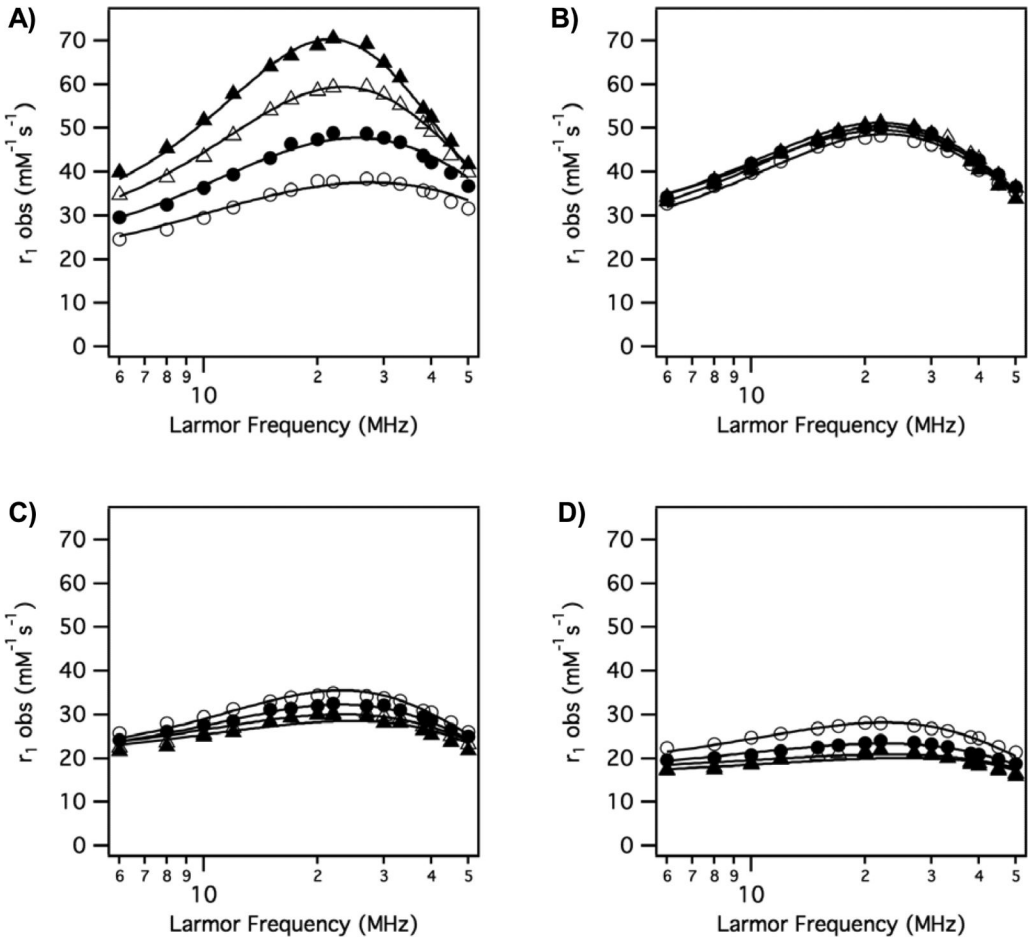

Figure 7.

Representative variable temperature (t = 35 °C (open circles); t = 25 °C (filled circles); t = 15 °C (open triangles); t = 5 °C (filled triangles)) NMRD with solid lines as fits to the data as described in the text. A) **Gd4b**; B) **Gd1c**; C) **Gd7a**; D) **Gd2c**

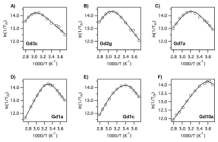

Figure 8.
Reduced O-17 T2 relaxation rates versus reciprocal temperature (symbols) and fits to estimate water exchange parameters determined in the absence of HSA. A) **Gd3c**; B) **Gd2g**; C) **Gd7a**; D) **Gd1a**; E) **Gd1c**; F) **Gd10a**

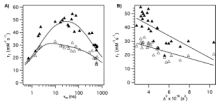

Figure 9.

A) Relaxivity of complexes in HSA solution at 37 °C plotted versus measured water residency time at 37 °C with data at 0.47T (filled symbols) and 1.4T (open symbols). Solid lines are curves generated using the mean molecular parameters listed in Table 1. B) Relaxivity of complexes in HSA solution at 37 °C plotted versus measured transient zero field splitting parameter Δ^2, a measure of electronic relaxation rate, with data at 0.47T (filled symbols) and 1.4T (open symbols). Solid lines are linear regressions.

Table 1

Molecular parameters derived from simultaneous fitting of variable temperature NMRD of albumin-bound gadolinium complexes. See text for details. Numbers in parentheses represent one standard deviation. RSD = relative standard deviation.

	τ_R (ns)	τ_m^{310} (ns)	τ_v (ps)	$\Delta H^{\ddagger}$ (kJ/mol)	Δ^2 (10^{18} s^{-2})	F^2
Gd1a	4.3 (0.2)	108 (14)	18 (2)	42.2 (2.5)	2.80 (0.14)	0.49 (0.02)
Gd1b	3.7 (0.2)	34.1 (6.7)	22 (3)	42.3 (4.2)	3.39 (0.12)	0.46 (0.01)
Gd1c	4.3 (0.2)	16.4 (1.8)	19 (2)	43.7 (2.8)	3.23 (0.09)	0.56 (0.01)
Gd1d	5.1 (0.2)	49.2 (2.5)	19 (1)	56.2 (1.2)	3.85 (0.07)	0.59 (0.01)
Gd1e	4.2 (0.2)	19.8 (2.6)	20 (2)	31.6 (3.3)	3.45 (0.08)	0.54 (0.01)
Gd1f	5.7 (0.2)	75.3 (.57)	18 (1)	41.3 (1.6)	3.97 (0.11)	0.68 (0.01)
Gd1g	4.7 (0.2)	9.8 (0.7)	18 (1)	43.3 (2.4)	3.56 (0.09)	0.54 (0.01)
Gd1h	4.3 (0.2)	37.6 (4.3)	21 (2)	47.9 (2.5)	3.93 (0.10)	0.52 (0.01)
Gd1i	3.8 (0.2)	24.0 (3.7)	21 (3)	47.9 (3.5)	3.36 (0.11)	0.46 (0.01)
Gd1j	3.9 (0.2)	64.7 (8.9)	21 (2)	40.1 (2.8)	3.33 (0.11)	0.48 (0.01)
Gd2b	7.6 (1.9)	441 (67)	17 (3)	31.3 (3.0)	4.47 (0.73)	0.62 (0.14)
Gd2c	11.6 (6.5)	579 (99)	18 (5)	30.9 (3.4)	5.97 (1.68)	0.8 (0.34)
Gd2d	11.4 (5.9)	570 (92)	17 (4)	30.6 (3.2)	5.71 (1.46)	0.8 (0.32)
Gd2f	13.8 (7.3)	536 (91)	18 (4)	23.9 (2.9)	6.22 (1.57)	0.8 (0.32)
Gd3a	7.7 (3.0)	499 (108)	21 (3)	10.8 (2.9)	7.9 (2.2)	0.8 (0.31)
Gd3c	7.2 (1.9)	612 (86)	28 (7)	13.4 (2.1)	10.4 (2.5)	0.72 (0.20)
Gd3f	5.0 (0.6)	574 (74)	28 (3)	33.3 (4.6)	7.1 (1.0)	0.53 (0.09)
Gd4a	20 (9.8)	0.7 (0.1)	26 (3)	34.9 (2.4)	5.56 (0.24)	0.48 (0.01)
Gd4b	17.2 (6.2)	1.9 (0.1)	23 (2)	30.5 (2.7)	4.20 (0.10)	0.62 (0.01)
Gd4c	11.0 (1.9)	2.4 (0.1)	25 (2)	33.8 (2.9)	4.32 (0.11)	0.61 (0.01)
Gd7a	6.2 (1.4)	281 (71)	17 (3)	23.2 (4.1)	4.82 (0.72)	0.60 (0.12)
Gd8a	8.0 (2.1)	370 (60)	16 (3)	32.1 (3.2)	4.84 (0.75)	0.66 (0.14)
Gd9a	7.0 (2.7)	1.4 (0.1)	30 (6)	27.4 (4.1)	4.94 (0.36)	0.53 (0.01)
Gd10a	5.6 (1.0)	2.1 (0.1)	24 (3)	31.2 (4.1)	4.00 (0.15)	0.69 (0.01)
Gd11a	4.2 (0.2)	54 (12)	19 (2)	24.5 (3.9)	3.20 (0.13)	0.69 (0.02)
Mean	7.5	199	21	33.9	4.74	0.61
Std dev	4.4	238	4	10.5	1.75	0.11
RSD	58%	120%	19%	31%	37%	18%

Table 2

Water exchange parameters determined from variable temperature O-17 NMR relaxation data on gadolinium complexes in the absence of protein.

	Gd1a	Gd1c	Gd2f	Gd3f	Gd7a	Gd10a
τ_m^{310} (ns)	85 (17)	46.5 (3.3)	622 (51)	777 (64)	330 (50)	9.1 (0.4)
$\Delta H^{\ddagger}$ (kJ/mol)	56.1 (2.9)	56.4 (0.7)	34.4 (1.9)	22.7 (2.0)	31.6 (3.2)	26.1 (1.3)